NUMERICAL MODELLING OF DESICCATION PROCESSES IN CLAYEY SOILS

H.U. Levatti, P.C. Prat and A. Ledesma

Technical University of Catalonia, Barcelona, Spain

ABSTRACT: *Desiccation processes in clayey soils involve a gradual moisture content loss induced by evaporation from the soil surface. The desiccation process, mainly governed by very nonlinear hydraulic properties, has an influence on the mechanical behaviour of the soil because the material tends to shrink, thus inducing changes in the stress fields. To understand this process one needs to solve the coupled hydraulic-mechanical problem. In this paper the formulation (including the unsaturated soil equilibrium and the mass balance equations) and some initial results of a numerical finite element code that solve the boundary value problem are presented. The state variables used in the model are the net stress (total stress) and the suction (negative pore water pressure). For the mechanics part, a non-linear elasticity model based on the state surface concept is chosen, while for the hydraulics problem, Darcy's law, including unsaturated flow, is used. To relate negative pore water pressure to the degree of saturation the van Genuchten equations are used.*

1   INTRODUCTION

Present models available in the literature dealing with drying cracks in soils do not include all aspects of the problem in an integral manner. Usually they solve only separately partial aspects such as occurrence and morphology of cracks, depth and spacing of cracks, consolidation and desiccation, shrinking-swelling, etc. (Aoki et al. 2002; Cheng 1993; Gordeyev 1993; Hallett and Newson 2005; Hallett et al. 1995; Hashin 1988; Kodikara et al. 2004; Konrad and Ayad 1997; Peron et al. 2009; Prat et al. 2002; Rodríguez et al. 2007; Sadda et al. 1994; Selvadurai and Mahyari 1998; Towner 1987; Yoshida and Adachi 2004). In this paper a general framework is presented using a FEM (Galerkin's method) combining continuum mechanics and unsaturated soil mechanics to simulate and solve problems of shrinkage and eventually cracking due to drying in soils in a consistent manner (Levatti et al. 2007; Prat et al. 2008). Continuum mechanics contributes with two equations: equilibrium and water balance. Unsaturated soil mechanics appears with the state surface concept, Darcy's law and the water retention curve.

Two state variables are adopted in this model: net stress and suction. The model is hydro-mechanically coupled: for the mechanics part, a non-linear elasticity model is chosen, while for the hydraulics problem, Darcy's law, including unsaturated flow, is used.

Some initial results are presented in this paper after a very concise description of the theoretical formulation.

2   HYDRO-MECHANICAL MODEL

Two state stress variables are adopted in this model: net stress $\boldsymbol{\sigma}^*$ and suction s:

$$\boldsymbol{\sigma}^* = \boldsymbol{\sigma} - p^a \mathbf{1} \tag{1}$$

$$s = p^a - p \tag{2}$$

With the assumption that atmospheric pressure p^a is constant and equal to zero, the state variables become the total stress $\boldsymbol{\sigma}$ and the negative pore water pressure p:

$$\boldsymbol{\sigma}^* = \boldsymbol{\sigma} \quad \text{and} \quad s = -p \tag{3}$$

Under the assumptions of small-strain theory, isothermal equilibrium and negligible inertial forces, we obtain the following balance equations. First, the linear momentum balance equation for a two phase medium, where ρ is the density and $\mathbf{g}$ is the gravity vector:

$$\nabla \cdot \boldsymbol{\sigma} + \rho \mathbf{g} = 0 \tag{4}$$

Second, the water mass balance equation, where ρ^w is the water density, $\mathbf{q}$ is Darcy's velocity, n the porosity and S_r the degree of saturation:

$$\nabla \cdot (\rho^w \mathbf{q}) + \frac{\partial}{\partial t}(\rho^w n S_r) = 0 \tag{5}$$

We can summarize the coupled problem through the next system of differential equations:

$$\begin{cases} \mathbf{K}\dfrac{\partial \overline{\mathbf{u}}}{\partial t} + \mathbf{Q}\dfrac{\partial \overline{\mathbf{p}}}{\partial t} - \mathbf{f}^u = \mathbf{0} \\[3mm] \mathbf{P}\dfrac{\partial \overline{\mathbf{u}}}{\partial t} + \mathbf{S}\dfrac{\partial \overline{\mathbf{p}}}{\partial t} + \mathbf{H}\overline{\mathbf{p}} - \mathbf{f}^p = \mathbf{0} \end{cases} \tag{6}$$

where $\overline{\mathbf{u}}$ and $\overline{\mathbf{p}}$ are, respectively, the nodal displacements and the nodal pore pressure vectors; $\mathbf{K}$, $\mathbf{S}$, $\mathbf{H}$ are the stiffness, compressibility and permeability matrices respectively and $\mathbf{Q}$, $\mathbf{P}$ are coupling matrices; $\mathbf{f}^u$, $\mathbf{f}^p$ are the nodal force and nodal flow vectors respectively; all resulting from the FEM approach:

$$\mathbf{K} = \int_\Omega \mathbf{B}^T \mathbf{D} \mathbf{B} d\Omega \tag{7}$$

$$\mathbf{Q} = \frac{1}{3K^s} \int_\Omega \mathbf{B}^T \mathbf{D} \mathbf{m} \mathbf{N}_p \overline{\mathbf{p}} d\Omega \tag{8}$$

$$\mathbf{P} = \int_\Omega \left(\mathbf{N}_p\right)^T S_r \mathbf{m}^T \mathbf{B} d\Omega + \int_\Omega \left(\mathbf{N}_p\right)^T n \frac{\partial S_r}{\partial \boldsymbol{\sigma}^*} \mathbf{C} \mathbf{B} d\Omega \tag{9}$$

$$\mathbf{S} = \int_\Omega \left[\frac{nS_r}{K^w}(\mathbf{N}_p)^T \mathbf{N}_p + nC_s(\mathbf{N}_p)^T \mathbf{N}_p \right] d\Omega \tag{10}$$

$$\mathbf{H} = \int_\Omega \left(\nabla \mathbf{N}_p\right)^T \mathbf{K}^P(S_r) \nabla \mathbf{N}_p d\Omega \tag{11}$$

$$\mathbf{f}^u = \int_\Omega (\rho_s(1-n) + S_r n \rho_w) \mathbf{N}_u^T \mathbf{g} d\Omega + \int_\Gamma \mathbf{N}_u^T \mathbf{t} d\Gamma \tag{12}$$

$$\mathbf{f}^p = \int_\Omega \rho_w \left(\nabla \mathbf{N}_p\right)^T \mathbf{K}^P(S_r) \mathbf{g} d\Omega - \int_\Gamma \mathbf{N}_p^T \mathbf{q}^w d\Gamma \tag{13}$$

where **C** and **D** are the stiffness and compliance tensors respectively; **B** is the matrix relating strains to displacements; $\mathbf{N}_p$ and $\mathbf{N}_u$ are the shape functions for pore pressures and displacements respectively; $\mathbf{m} = (1,1,0)$ is the generalized identity tensor in vector form for 2D analysis; C_s is the specific water content; $\mathbf{K}^P$ is the permeability tensor; K^s is the bulk modulus for suction; K^w is the water bulk modulus; **t** and $\mathbf{q}^w$ are the imposed nodal force and flow vectors respectively.

The algebraic system of equations that results from this formulation is highly nonlinear and non-symmetric, in general. For this reason solving the problem requires the use of iterative strategies. The first equation in (6) is the mechanical part and the second one is the hydraulic part.

3 UNSATURATED SOIL MECHANICS CONCEPTS

For the hydro-mechanical formulation two constitutive models are needed. The mechanical constitutive model, Eq. (14), is written in terms of state surfaces (Alonso et al. 1990; Lloret and Alonso 1985; Matyas and Radhakrishna 1968) whereas for the hydraulic constitutive model, including unsaturated flow, Eq. (15), Darcy's law is used. The models can be written as follows:

$$\varepsilon_v = -\frac{e}{1+e_0} = a_1 \ln(\sigma_m + a_4) + a_2 \ln\left(\frac{p + p_{ref}}{p_{ref}}\right) + a_3 \left[\ln(\sigma_m + a_4) \ln\left(\frac{p + p_{ref}}{p_{ref}}\right)\right] \tag{14}$$

$$\mathbf{q} = -\mathbf{K}(S_r)\cdot(\nabla p - \rho^w \mathbf{g}) \tag{15}$$

where ε_v is the volumetric strain; σ_m is the mean stress; e and e_0 are the current and initial void ratios; a_1, a_2, a_3, a_4 are state surface constants; p is the negative pore water pressure; and p_{ref} is a reference pressure.

Furthermore, we need to express the relation between suction and degree of saturation. For the purpose of this paper the following relation (van Genuchten 1980) has been chosen:

$$S_r = \left[1 + \left(\frac{p}{P_0 f_n}\right)^{\frac{1}{1-\lambda}}\right]^{-\lambda} \tag{16}$$

where S_r is the degree of saturation, λ is a material parameter, P_0 is the air entry value at the reference porosity n_0 and f_n is a function of porosity and material parameters.

4 RESULTS OF THE NUMERICAL MODEL

The results of six simulations on a sample of 20×20 cm in size are presented below. The boundary conditions are described schematically in Figure 1.
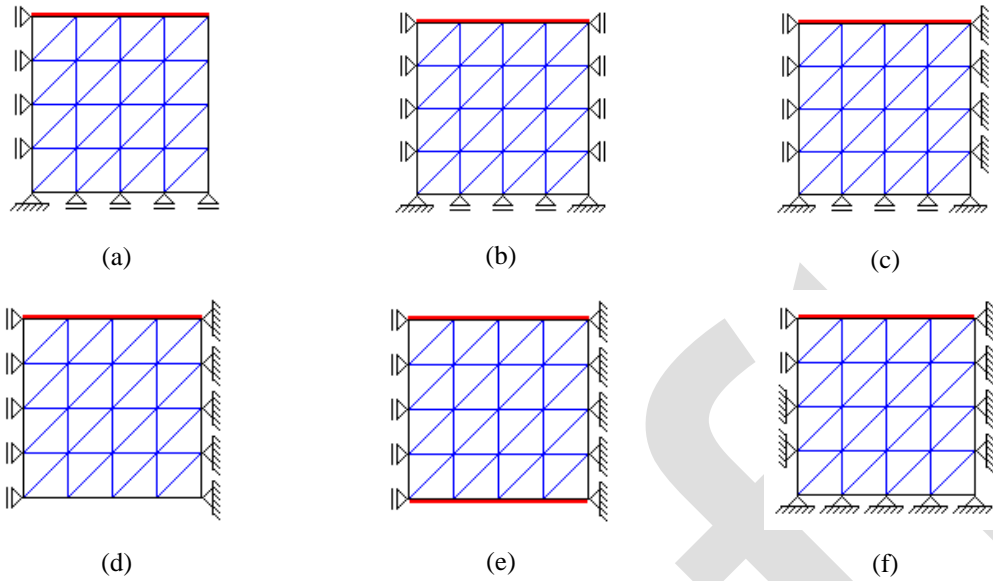
Fig. 1. Schematic representation of boundary conditions for displacements and pore water pressure.

This corresponds to a section of a cylindrical sample of 40 cm in diameter and a depth of 20 cm that because of symmetry can be analyzed as a plane problem (2D). The pore water pressure is applied either on the top (Figure 1a, b, c, d and f) or on the top and bottom of the sample (Figure 1e) and it is equal to -59 MPa during a simulation of a 40 days drying period. The six schemes shown in Figure 1 are analyzed with five different displacement boundary conditions and two different pore water pressure boundary conditions.

Boundary conditions such as the ones depicted in Figures 1a,b only produce compressive stresses in this model during desiccation, as shown in Figure 2, where a reduction on volume and hence on the porosity of the medium can be noticed. Of course this kind of stress field cannot produce any crack in the soil mass: only shrinkage takes place.

Figure 2 shows the relation between strain and stress at three reference points for the first and second schemes depicted in Figure 1. The final results shown in Figure 2a are consequence of the high value of pressure imposed that makes the continuum much stiffer at the top than at the bottom. Because the vertical displacement is restricted, the soil mass tends to shrink horizontally, shrinkage increasing with depth.

Figure 2a (corresponding to Figure 1a) shows that strain and stress increase with depth not only in final values but also during the drying process. For the scheme shown in Figure 1b, the boundary conditions are such that the horizontal strain and stress are zero, and the vertical strain and stress are the only stresses that change during desiccation, making this is rather a 1D case (as shown in Figure 2b).

Figure 3 shows the strain and stress fields obtained using the scheme depicted in Figure 1c. With these boundary conditions, tensile stresses appear at the top of the sample and decrease with depth until they reach a zero value and become compressive until reaching the maximum depth. We can predict with this model that the first desiccation crack is likely to appear at the contact between the tray and the soil sample and most probably at the top of the sample. This fact was established experimentally in a large desiccation program test. Figure 3a shows the relation between horizontal and vertical stresses vs. horizontal and vertical strains at the top, bottom and mid-depth nodes.
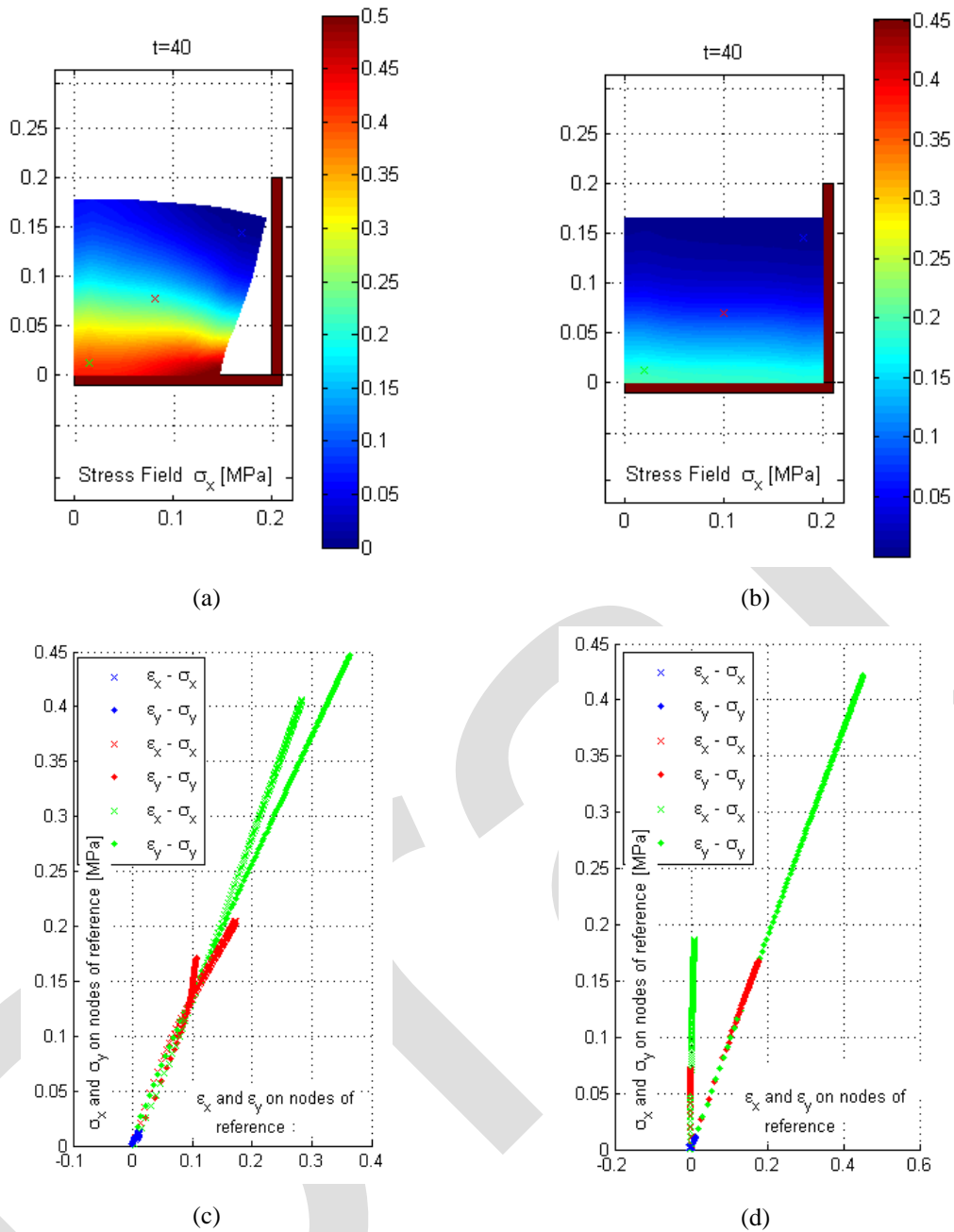
Fig. 2. Horizontal stress field during desiccation process (schemes *a* and *b* in Fig. 1)

Figure 4 shows the results of imposing the boundary conditions shown in Figure 1b to a sample with a crack, as shown in Figure 4b. Figure 4a depicts the strain-stress relation at three different points of the sample, showing the maximum stress at the crack tip. Evolution of pore water pressure and porosity at a point near the crack opening are shown in Figures 4c,d. This kind of evolution of pore water pressure is typical in problems of flow in unsaturated media.

Figure 5 shows the final state of the analysis corresponding to the boundary conditions illustrated in Figures 1d,e,f. Figures 5a,c,e show the final pore water pressure field whereas Figures b,d,f show the final horizontal stress field.

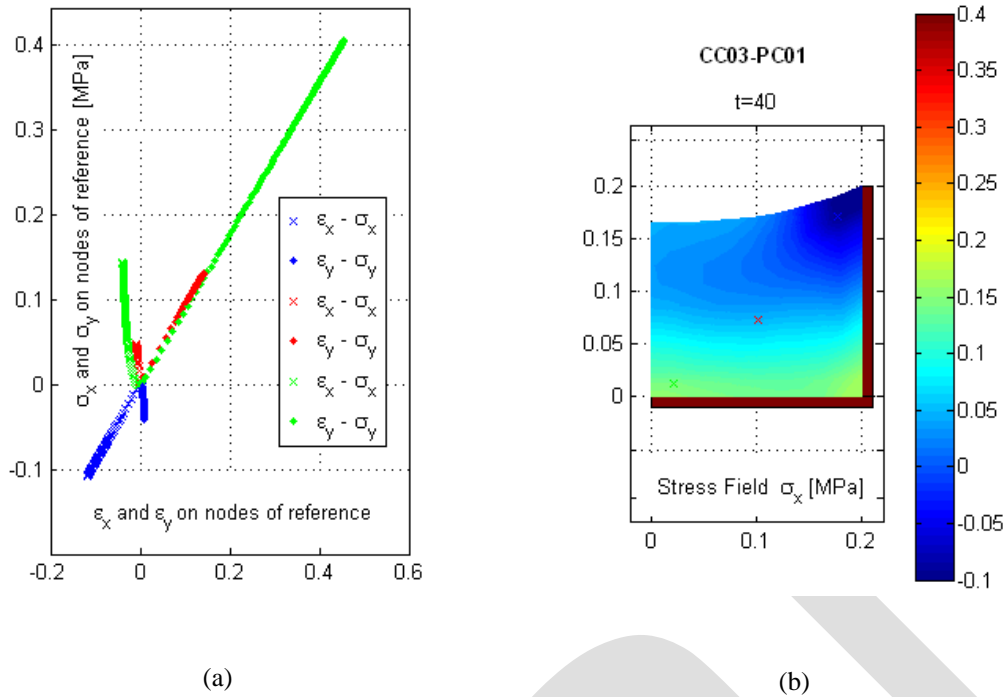(a)   (b)

Fig. 3. Stress and strain evolution during desiccation (scheme *c* in Fig. 1)

In the first case shown in this pictures (Figures 5a,b) one can see the curling effect produced because the vertical displacement is unrestricted at the bottom of the sample. In this case, like in the sample shown in Figure 3, horizontal tensile stresses do appear at the top right-hand corner. At the bottom corner, horizontal tensile stresses also appear but its value is less than at the top.

Figures 5c,d represent the same case but imposing pore water pressure at the top and the bottom of the sample. The effect of this boundary condition is that the stress field is symmetric respect to a horizontal axis at mid-depth of the sample and in the same way the pore water pressure field is symmetric too. Deformation of the soils mass is less than in the previous case because the new pore water pressure condition gives major stiffness to the sample.

Figures 5e,f shows the final state obtained with the more complex boundary conditions shown in Figure 1f. Because the boundary conditions are not symmetric, the pore water pressure and stress fields are non-symmetric as well.

5   CONCLUSIONS

The paper presents a general formulation to analyse the process of desiccation in clayey soils. The formulation is based on the general hydro-mechanical coupled equations of an unsaturated material. Results using a 2D version of this formulation, implemented in a Matlab environment, have been described in the paper. A state surface approach was considered for the mechanical constitutive law, whereas the conventional unsaturated flow equation was adopted for the hydraulic problem.
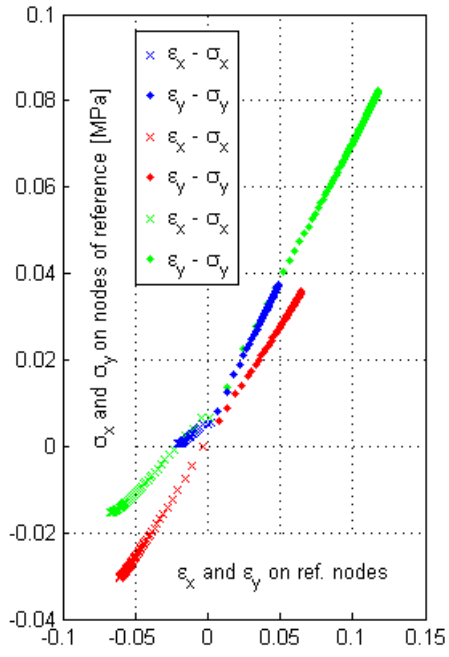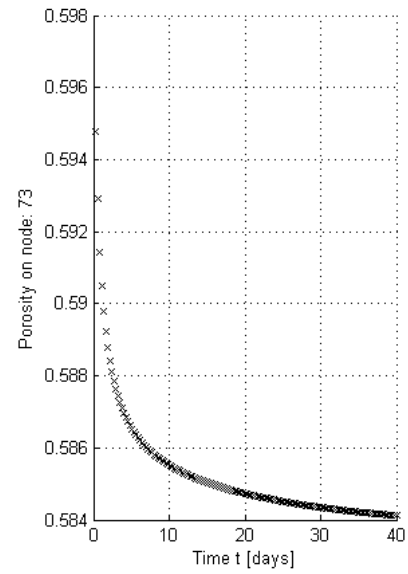
(a)
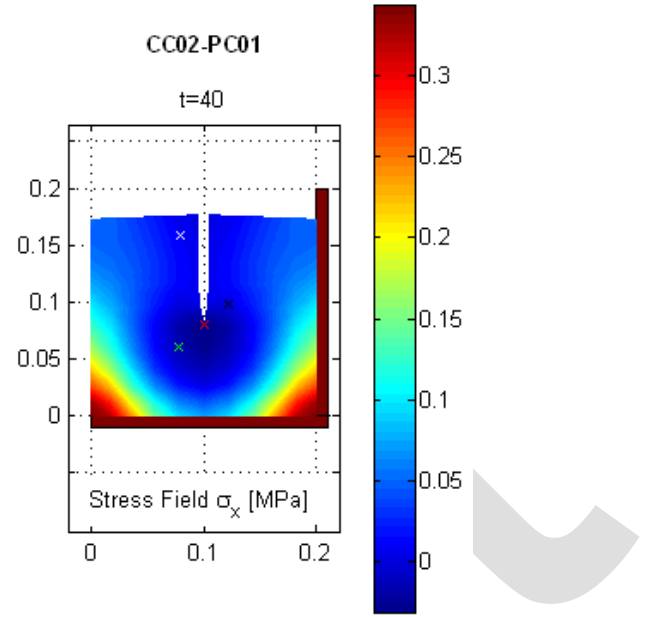
(b)
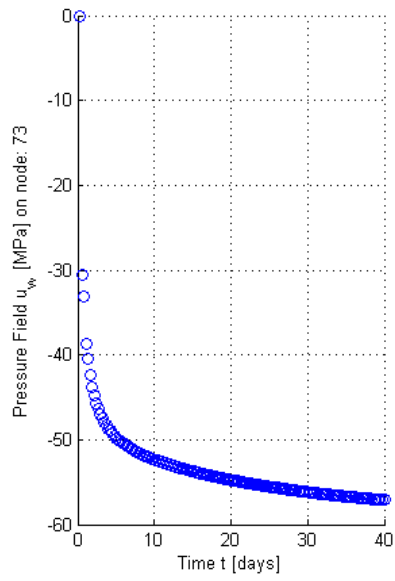
(c)

(d)

Fig. 4. Stress, strain, pore water pressure and porosity evolution during desiccation on a sample with a crack (scheme *b* in Fig. 1)
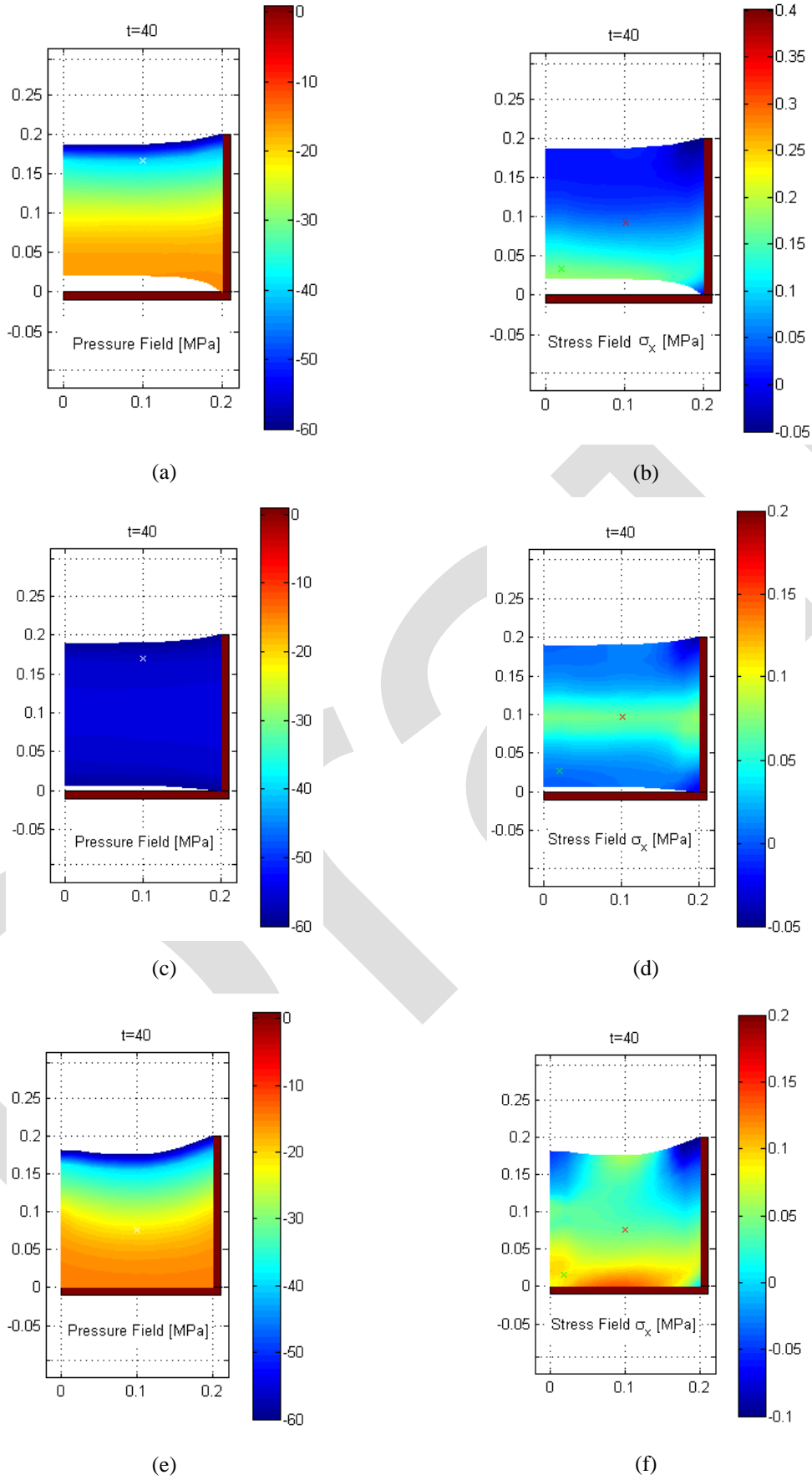
Fig. 5. Stress and strain evolution during desiccation (schemes *d*, *e*, and *f* in Fig. 1)

Boundary conditions have a fundamental influence on the stress-strain behaviour of the soil mass under desiccation process. There are boundary conditions that do not produce any tensile stress state and therefore no crack formation is possible. Boundary conditions change during the desiccation process and this fact has consequences on the behaviour of the soil mass. Taken into account these changes during the desiccation process is a highly complicated task, still under development. Of course, if during drying crack formation and propagation is included, changes in the field variables will be more complex and pore water pressure conditions will change accordingly.

There is a strong interaction between the hydraulic and mechanics phenomena that is important to take into account. This hydro-mechanical coupling allows discovering the main features that play a fundamental role in this complex phenomenon.

REFERENCES

Alonso, E.E., Gens, A., and Josa, A. 1990. A constitutive model for partially saturated soils. Géotechnique, **40**: 405-430.

Aoki, K., Hai Dong, N., Kaneko, T., and Kuriyama, S. 2002. Physically Based Simulation of Cracks on Drying 3D Solid. *In* 10th Pacific Conference on Computer Graphics and Applications (PG'02). Tsinghua University, Beijing. October 9-11.

Cheng, C.H. 1993. Crack models for a transversely isotropic medium. J. Geophysical Research, **98**(B1): 675-684.

Gordeyev, Y.N. 1993. Growth of a crack produced by hydraulic fracture in poroelastic medium. Int. J. Rock Mech. Min. Sci. & Geomech. Abstr., **30**(3): 233-238.

Hallett, P.D., and Newson, T.A. 2005. Describing soil crack formation using elastic-plastic fracture mechanics. European Journal of Soil Science, **56**: 31-38.

Hallett, P.D., Dexter, A.R., and Seville, J.P.K. 1995. The application of fracture mechanics to crack propagation in dry soil. European Journal of Soil Science, **46**(4): 591-599.

Hashin, Z. 1988. The differential scheme and its application to cracked materials. J. Mech. Phys. Solids, **36**(6): 719-734.

Kodikara, J.K., Nahlawi, H., and Bouazza, A. 2004. Modeling of curling in desiccation clay. Canadian Geotechnical Journal, **41**: 560-566.

Konrad, J.-M., and Ayad, R. 1997. An idealized framework for the analysis of cohesive soils undergoing desiccation. Canadian Geotechnical Journal, **34**: 477–488.

Levatti, H.U., Prat, P.C., and Ledesma, A. 2007. Numerical modelling of formation and propagation of drying cracks in soils. *In* Computational Plasticity IX (COMPLAS-IX). *Edited by* E. Oñate, D.R.J. Owen, and B. Suárez. Barcelona. CIMNE, Vol.2, pp. 840-843.

Lloret, A., and Alonso, E.E. 1985. State surfaces for partially saturated soils. *In* XI Int. Conf. Soil Mechanics and Foundation Engineering. San Francisco. Balkema, pp. 557-562.

Matyas, E.L., and Radhakrishna, H.S. 1968. Volume change characteristics of partially saturated soils. Géotechnique, **18**(4): 432-448.

Peron, H., Delenne, J.Y., Laloui, L., and El Youssoufi, M.S. 2009. Discrete element modelling of drying shrinkage and cracking of soils. Computers & Geotechnics, **36**: 61-69.

Prat, P.C., Ledesma, A., and Cabeza, L. 2002. Drying and cracking of soils: numerical modeling. *In* Numerical Models in Geomechanics VIII. Swets & Zielinger. pp. 705-711.

Prat, P.C., Ledesma, A., Lakshmikantha, M.R., Levatti, H.U., and Tapia, J. 2008. Fracture mechanics for crack propagation in drying soils. *In* IACMAG 12. *Edited by* D.N. Singh. Goa, India. IIT Mumbai, pp. 1060-1067.

Rodríguez, R.L., Sánchez, M.J., Ledesma, A., and Lloret, A. 2007. Experimental and numerical analysis of a mining waste desiccation. Canadian Geotechnical Journal, **44**: 644-658.

Sadda, A., Bianchini, G.F., and Liang, L. 1994. Cracks, bifurcation and shear bands propagation in saturated clays. Géotechnique, **44**(1): 35-64.

Selvadurai, A.P., and Mahyari, A.T. 1998. Computational modelling of steady crack extension in poroelastic media. Int. J. Rock Mech. Min. Sci. & Geomech. Abstr., **35**(34-35): 4869-4885.

Towner, G.D. 1987. The mechanics of cracking of drying clay. Journal of Agricultural Engineering Research, **36**: 115-124.

van Genuchten, M.T. 1980. Closed-form equation for predicting the hydraulic conductivity of unsaturated soils. Soil Science Society of America Journal, **44**(5): 892-898.

Yoshida, S., and Adachi, K. 2004. Numerical analysis of crack generation in saturated deformable soil under row-planted vegetation. Geoderma, **120**: 63-74.